Analysis of Compression-induced Auto-ignition Combustion Characteristics of HCCI and ATAC Using the Same Engine

Akira Iijima, Hideo Shoji*
Nihon University,
8-14, Kanda-Surugadai 1-chome, Chiyoda-ku, Tokyo 101-8308, Japan

Controlled Auto-ignition (CAI) combustion processes can be broadly divided between a CAI process that is applied to four-cycle engines and a CAI process that is applied to two-cycle engines. The former process is generally referred to as Homogeneous Charge Compression Ignition (HCCI) combustion and the later process as Active Thermo-Atmosphere Combustion (ATAC). The region of stable engine operation differs greatly between these two processes, and it is thought that the elucidation of their differences and similarities could provide useful information for expanding the operation region of HCCI combustion. In this research, the same two-cycle engine was operated under both the ATAC and HCCI combustion processes to compare their respective combustion characteristics. The results indicated that the ignition timing was less likely to change in the ATAC process in relation to changes in the fuel octane number than it was in the HCCI combustion process.

Key Words : Combustion, Auto-ignition, Octane Number, HCCI, ATAC

Nomenclature

ε : Effective compression ratio [$-$]
ϕ : Intake equivalence ratio [$-$]
η_S : Scavenging efficiency [$-$]
θ : Crank angle [deg.]
HRR : Heat release rate [J/deg.]
L : Corrected delivery ratio [$-$]
N : Engine speed [rpm]
P : In-cylinder pressure [MPa]
WOT : Wide open throttle
RH : Alkane fuels
R : Alkyl radical
ROO : Alkylperoxy radical
QOOH : Alkylhydroperoxide
OOQOOH : Peroxyalkylhydroperoxide
Sp : Instantaneous piston speed [m/sec]
T_{EGR} : EGR gas temperature [K]
Tex : Exhaust gas temperature [K]

Tsc : Scavenging temperature [K]
Tsp : Spark plug washer temperature [K]
Tmax : Maximum in-cylinder gas temperature [K]

1. Introduction

Homogeneous Charge Compression Ignition (HCCI) engine (Thring, 1989 ; Christensen et al., 1997 ; Lee et al., 2004) has attracted much interest because it achieves clean combustion with an ultra-low NOx level and no soot emission when operated under a non-throttled, lean-burn condition at an optimized compression ratio.

Examples of gasoline-fueled HCCI engines include four-cycle, high-compression-ratio engines that adopt a compression ignition combustion system (Aoyama et al., 1996) and two-cycle engines that operate under compression ignition combustion at partial load. This type of combustion process is called by different names such as Active Thermo-Atmosphere Combustion (ATAC) or Activated Radicals (AR) combustion (Onishi et al.,

* Corresponding Author,
 E-mail : shoji@mech.cst.nihon-u.ac.jp
 TEL : +81-3-3259-0739; **FAX** : +81-3-3259-0739
 Nihon University, 8-14, Kanda-Surugadai 1-chome, Chiyoda-ku, Tokyo 101-8308, Japan. (Manuscript **Received** June 25, 2005; **Revised** May 29, 2006)

Because reaction (2) is a chain propagation step, acceleration of the reaction ceases in the negative temperature coefficient (NTC) region. Subsequently, the gradual reaction rate, compression by piston motion and other factors cause the temperature to rise to around 1100 K. At that temperature level, reaction (3) occurs, producing a large quantity of OH radicals (blue flame region) and leading to autoignition. In relation to the temperature rise, two-stage ignition occurs owing to the progression from reaction (1) to reaction (3), i.e., from a cool flame to NTC to autoignition.

With HCCI combustion, the premixed mixture begins to be compressed from a point below the cool flame temperature. Consequently, depending on the fuel used, HCCI combustion follows a low-temperature oxidation process in which a cool flame occurs, passes through the NTC region owing to the resultant temperature rise, and then proceeds to autoignition due to the occurrence of reaction (3) in the vicinity of 1100 K.

The degree to which reactions (1) and (2) occur depends not only on the temperature, but also differs greatly according to the molecular structure of the fuel. The reason is that the tendency for internal isomerization to occur varies depending on the molecular structure. Consider, for example, the difference between n-heptane and iso-octane. Straight-chain n-heptane easily undergoes internal isomerization of its six- or seven-membered ring with low strain energy on account of its molecular structure. Owing to reaction (1) in Fig. 1, chain branching readily takes place. On the other hand, in the case of iso-octane with its side chains, internal isomerization of its five-membered ring with high strain energy is more apt to occur compared with the six- or seven-membered rings. Moreover, in the case that internal isomerization of the five-membered ring occurs, QOOH tends to decompose $(QOOH \Rightarrow Q + HO2)$ relatively stably to produce HO2, and chain branching is not apt to occur. Consequently, n-heptane which passes through six- or seven-membered ring structures with low strain energy and results in chain branching is more likely to produce cool flame reactions. These observations explain why

heat release due to a cool flame is clearly detected in HCCI combustion of n-heptane, but is nearly indiscernible in the case of iso-octane.

3. Experimental Equipment and Procedure

The test engine used in this study was a two-cycle air-cooled single-cylinder engine having the specifications shown in Table 1. The engine operating conditions used in this work were broadly divided as indicated below and will be referred to in the following discussion as ATAC and HCCI, respectively.

(1) ATAC : compression ignition combustion at partial load in a two-cycle engine
(2) HCCI : compression ignition combustion simulating HCCI combustion at WOT in a four-cycle engine

The test engine was operated under the ATAC process at partial load at an effective compression ratio of 8.7 : 1 and under the HCCI process at WOT and effective compression ratios of 8.7 : 1 and 15 : 1. Cylinder pressure data, heat release rate and radical light emission behavior were recorded and analyzed under each set of operating conditions.

The configuration of the test equipment used is outlined in Fig. 2, and the measurement positions are shown in Fig. 3. Light emission intensities of the radicals of interest were measured in the following way. Flame light in the combustion chamber was extracted by means of a quartz observation window installed in the top of the cy-

Table 1 Specifications of test engine

2-cycle Air Cooled SI Engine	
scavenging Type	Schn? le
Bore? Stroke	72?60 mm
Displacement	244 cm³
Effective Compression Ratio	8.7 : 1 (ATAC, HCCI) 15 : 1 (HCCI)
Test Fuels	PRF (RON 0, 30, 50, 60, 80, 100) Gasoline (91 RON)

linder head and introduced into a polychromator via an optical fiber cable having a core diameter of 1 mm. The light was separated into wavelengths of 395.2 nm (corresponding to HCHO), 329.8 nm (HCO) and 306.4 nm (OH), and the light emission intensity at each wavelength was measured with a photomultiplier (Shoji et al., 1992 ; 1993 ; Inoue et al., 2000 ; Suzuki et al., 2003). In order to investigate the overheated state of the engine and the operating conditions, measurements were made of the spark plug washer temperature (Tsp), scavenging temperature (Tsc) and exhaust gas temperature (Tex: about 40mm downstream from the exhaust port).
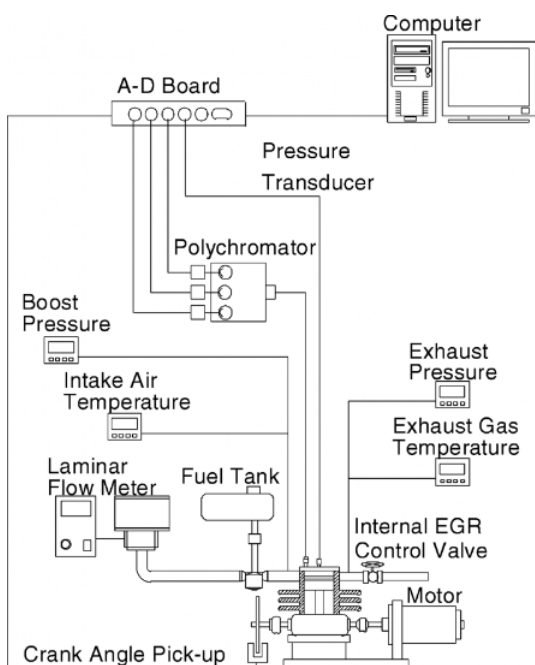

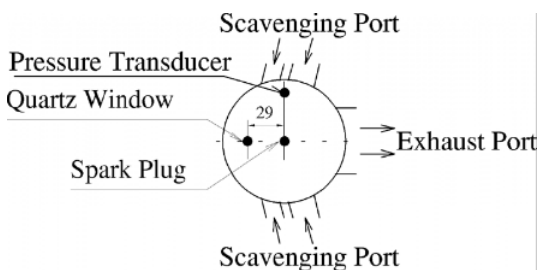**Fig. 2**   Configuration of test equipment

Fig. 3   Measurement positions and scavenging ports

4. Calculation Method

Numerical calculations of elementary reactions were performed using CHEMKIN 3.7 (AURORA Application) under dimensionless, adiabatic conditions and by applying the same volumetric change as that of the test engine. The following two types of reaction mechanisms were used, all of which were developed at the Lawrence Livermore National Laboratory (LLNL).

(1) n-heptane : 544 chemical species, 2446 elementary reactions (Curran et al., 1998a).

(2) primary reference fuels (PRF) : 1034 chemical species, 4238 elementary reactions (Curran et al., 2002 ; Curran et al., 1998b) (blended fuels of n-heptane and iso-octane)

5. Results and Discussion

5.1   Radical light emission behavior and mole fraction histories of chemical species under ATAC and HCCI combustion

Autoignited combustion was induced in this study at partial load under an effective compression ratio of $\varepsilon=8.7:1$ and an engine speed of approximately 2200 rpm. These conditions gave rise to autoignited combustion corresponding to ATAC at partial load in a two-cycle engine. As one example of ATAC characteristics, Figure 4 shows the waveforms measured at an engine speed of N=2500 rpm when n-heptane (0 RON) was used as the test fuel.

The heat release rate (HRR) waveform for ATAC combustion indicates that autoignition was reached (region A in Fig. 4) without any discernable sign of heat release attributable to the passage of a cool flame (Kaneko, 2001 ; Eng, 2002) prior to ignition. In general, increasing the throttle valve opening or reducing the engine speed causes misfiring in the ATAC process, making stable engine operation impossible. One reason for that in the case of a larger throttle valve opening is attributed to the resultant increase in scavenging efficiency which reduces the quantity of high-temperature combustion gas remaining in the cylinder. Reduc-

ing the engine speed, on the other hand, lowers the temperature of the residual gas, and the interaction of the two factors reduces the temperature at the onset of compression, making it impossible to reach the temperature level needed to induce autoignition. However, when a fuel with a low octane number was used, it was observed that a region existed under WOT and low speed conditions where autoignited operation of the engine was possible.

Figure 5 shows the waveforms measured at WOT and N=1000 rpm. Heat release presumably ascribable to the passage of a cool flame can be observed in the HRR waveform (region B) prior to ignition and a second heat release stage attributed to the hot flame is subsequently seen. This pattern indicates autoignited combustion corresponding to HCCI combustion in a four-cycle engine. Concurrent with the heat release attributed to the cool flame, the light emission intensity waveform of HCHO shows signs of faint light emission and degeneracy behavior (region C). It has been reported that light emission from a cool flame represents the luminescence of excited-state formaldehyde (HCHO) (Gaydon, 1957). It is assumed that this faint HCHO light emission signifies such light emission from a cool flame. As these results indicate, the reaction path can lead to autoignition under conditions where a cool flame is manifested even in a low temperature region at the onset of compression. The combustion that occurs in such cases is thought to be the same as HCCI combustion in a four-cycle engine. In other words, the difference between ATAC and HCCI combustion is attributed to variation in the low-temperature oxidation reaction (Pilling et al., 1997 ; Warnatz et al., 2001 ; Chevalier et al., 1990) characteristics of a hydrocarbon fuel resulting from changes in the cylinder temperature and pressure and in their time histories. That variation corresponds to changes in the degree of influence of the passage of a cool flame and NTC. It suggests that a good understanding of these characteristics can be useful in suppressing or promoting autoignition.

Figure 6 shows the results of calculations that simulated the experimental ATAC characteristics

ATAC - Experimental					
ε [-]	N [rpm]	φ [-]	throttle	L (ns) [-]	Fuel (RON)
8.7 : 1	2500	1.0	part throttle	0.5 (0.43)	n-heptane (0 RON)
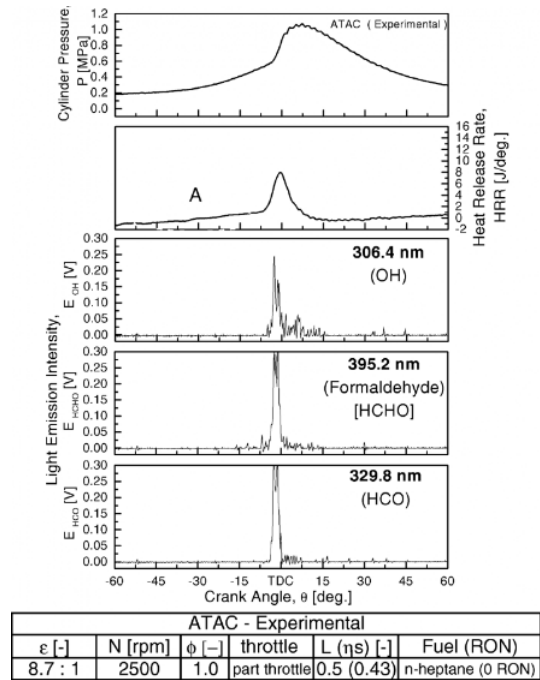
Fig. 4 Typical waveforms of ATAC （Experimental）

HCCI - Experimental				
ε [-]	N [rpm]	φ [-]	throttle	Fuel (RON)
8.7 : 1	1000	0.65	WOT	n-heptane (0 RON)
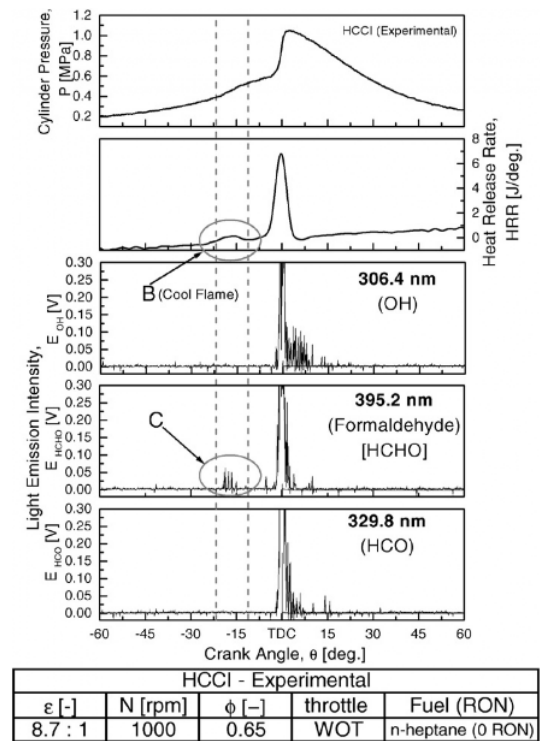
Fig. 5 Typical waveforms of HCCI （Experimental）

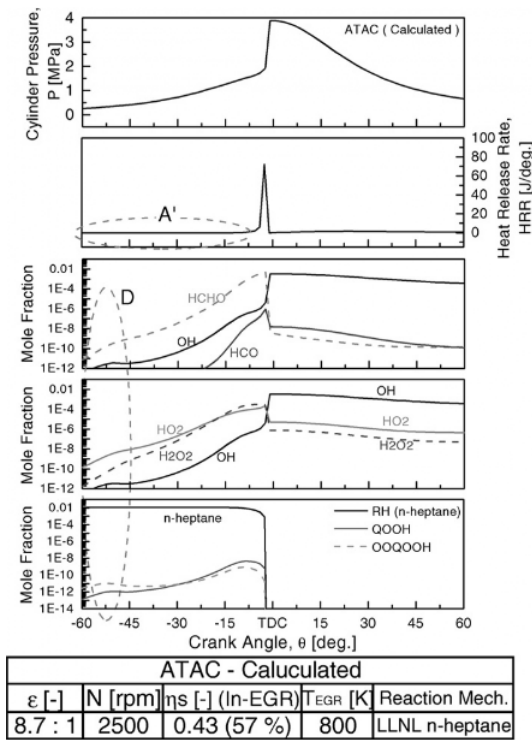**Fig. 6** Typical waveforms of ATAC
（Caluculated）

Fig. 7 Typical waveforms of HCCI
（Caluculated）

in Fig. 4. It is presumed that a large quantity of internal EGR gas is present in the ATAC process. Accordingly, the calculations were performed under the following hypotheses in order to take account of internal EGR.

（1）The internal EGR gas has a balanced composition of N2, O2, CO2 and H2 in the case of complete combustion of the fuel.

（2）The temperature of the internal EGR gas is 800 K.

Based on these hypotheses, the calculations were performed at a scavenging efficiency of $\eta_S=$ 0.43 （Internal EGR rate of In-EGR=57%）and under the assumption that residual gas, having the composition and temperature noted above, was perfectly mixed with the new intake air. In the ATAC simulation results in Fig. 6, neither the cylinder pressure waveform nor the HRR waveform shows any sign of a temperature rise attributable to a cool flame in region A' prior to the development of the hot flame.

However, looking at the mole fraction histories of the chemical species, weak peaks are observed in the vicinity of 50 deg. BTDC （region D in Fig. 6）. These peaks are believed to indicate the position where reactions corresponding to the passage of a cool flame occurred. Because their level is extremely low, however, the passage of a cool flame is not discernable in the HRR waveform.

Figure 7 presents the results of calculations that simulated the experimental HCCI characteristics in Fig. 5. In this case, heat release attributable to the passage of a cool flame can be observed. Concurrently, sharp peaks also appear in the mole fraction waveforms of the chemical species, and a notable increase is seen in HCHO （line B'）among the OH, HCHO and HCO radicals.

5.2 Influence of fuel octane number on ignition timing in ATAC and HCCI combustion

The results presented in the preceding subsection revealed a significant difference between ATAC

and HCCI combustion in that a cool flame was not manifested in the former process, whereas it was in the latter process. That difference was attributed to a difference in temperature at the onset of compression, among other factors. As the next step, the octane number of the fuel was varied and an investigation was made of the resultant effect on the autoignition tendency of the ATAC and HCCI combustion processes.

The influence of the octane number (RON) on the HRR waveforms is shown in Figs. 8 and 9 for ATAC and HCCI combustion, respectively. All of the waveforms are plotted in relation to a constant scavenging temperature (T_{SC}). However, when 80 RON fuel and gasoline were used, the engine could not be operated under HCCI combustion because of misfiring, so the corresponding waveforms are for a higher scavenging temperature where ignition was possible. Because a large quantity of internal EGR gas was present in the case of ATAC, the waveforms are also indicated for a constant exhaust temperature (T_{ex}) in addition to T_{SC}. Moreover, the subsequent results for HCCI combustion are all for an effective compression ratio of $\varepsilon = 15:1$ in order to achieve combustion more closely resembling the HCCI combustion process in a four-cycle engine.

As seen in Fig. 8, varying the octane number of the test fuel did not change the ignition timing appreciably in the ATAC process (arrow E). In contrast, the results for HCCI combustion in Fig. 9 indicate that varying the fuel octane number reduced the amount of heat released by the passage of a cool flame (arrow F) and substantially retarded the ignition timing (arrow G) compared with that seen for ATAC.

In other words, the octane number of the fuel had a marked effect on the ignition timing under HCCI operation, whereas its effect was small under ATAC operation.

As the reason for that difference, we can consider the differences in the respective temperature histories followed by the ATAC and HCCI combustion processes. With HCCI combustion, increasing the fuel octane number retarded ignition, which presumably can be attributed to the low-temperature reaction rate stemming from the
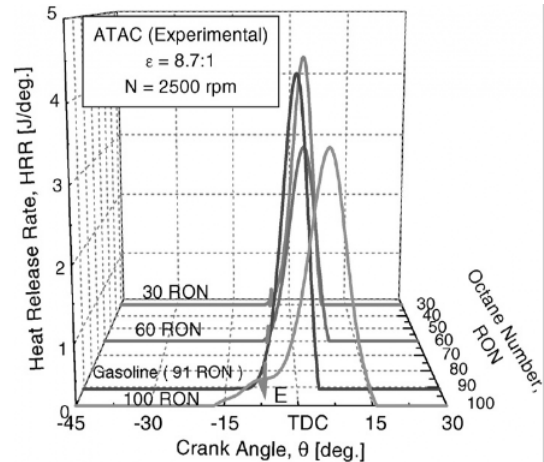

Fig. 8 Influence of octane number on HRR (ATAC-Experimental)
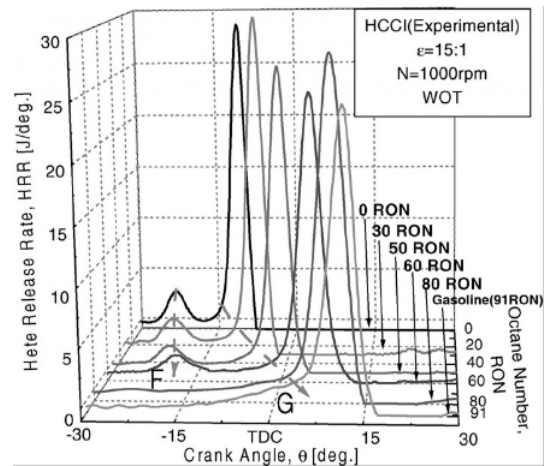
Fig. 9 Influence of octane number on HRR (HCCI-Experimental)

molecular structure, or in other words, the influence of a cool flame. In ATAC, a cool flame was not manifested even when a fuel with a low octane number was used, which is why little correlation is seen between the octane number and the change in ignition timing.

The following reasons can be considered for why a cool flame did not develop in ATAC.

(1) Because of the high engine speed in this process, the piston moves faster and compression by piston motion accounts for a larger proportion of the temperature rise, with the result that the

Fig. 10 Crank angle vs. instantaneous piston speed

cool flame is reduced by a corresponding extent.

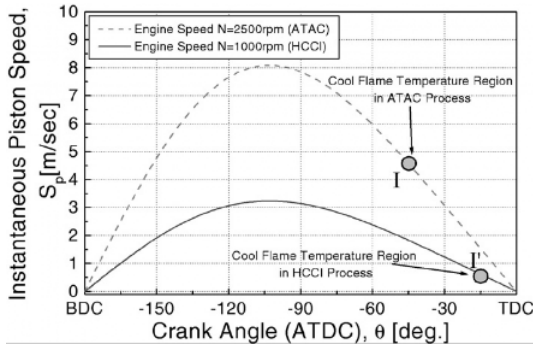（2）Because of the large quantity of residual gas, the oxygen concentration is low, making it difficult for oxidation to take place.

（3）The cylinder pressure is low at the time the combustion reactions pass through the cool-flame temperature region.

（4）Because the temperature at the onset of compression is raised by the residual gas, the combustion reactions pass through the cool-flame temperature region at a crank angle where the instantaneous piston speed is higher. As shown in Figure 10, the piston speed varies depending on the crank angle in piston engines. Consequently, as the temperature at the onset of compression rises, cool-flame reactions occur at an earlier crank angle, and the instantaneous piston speed at that point increases（see point I in Fig. 10）.

Next, we will discuss the respective calculated results for ATAC and HCCI combustion. Figure 11 shows the measured HRR waveforms obtained under ATAC operating conditions with the test fuels of varying octane numbers, and Fig. 12 shows the corresponding calculated results obtained for HCCI operating conditions. As is evident in both figures, the calculated results show nearly the same tendencies as the experimental data. It is clear that varying the fuel octane number had much less effect on the ignition timing in the ATAC process compared with HCCI combustion.

The fact that the ATAC process allows autoignition of fuels over a wide range of octane numbers also correlates with these results.
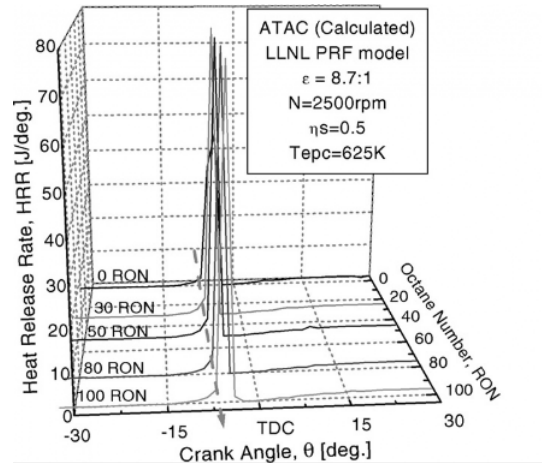
Fig. 11 Influence of octane number on HRR （ATAC-Calculated）
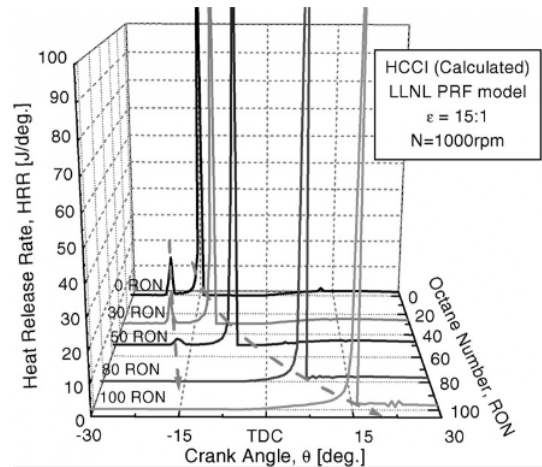
Fig. 12 Influence of octane number on HRR （HCCI-Calculated）

6. Conclusions

In this study, a two-cycle engine was used to compare the characteristics of Active Thermo-Atmosphere Combustion （ATAC）under partial load and Homogeneous Charge Compression Ignition （HCCI）combustion under a WOT condition that simulated HCCI combustion in a four-cycle engine. The results obtained have made the following points clear.

（1）With n-heptane（0 RON）as the test fuel, both the experimental and calculated heat release rate（HRR）waveforms showed evidence of the

passage of a cool flame under HCCI combustion but not under ATAC.

(2) In HCCI combustion with n-heptane (0 RON), faint light emission and degeneracy behavior were observed for HCHO at the time of heat release from a cool flame.

(3) In the ATAC process, the ignition timing did not change much in relation to the octane number of the fuel. In contrast, the use of a test fuel with a higher octane number in the HCCI combustion process reduced the heat release from a cool flame and also retarded the ignition timing.

(4) Auto-ignited combustion was strongly influenced by the temperature and pressure paths resulting from compression by piston motion and by their time-related changes.

References

Aoyama, T., Hattori, Y., Mizuta, J. and Sato, Y., 1996, "An Experimental Study on Premixed-Charge Compression-Ignition Gasoline Engine," SAE paper 960081.

Chevalier, C., Louessard, P., Müller, U. C. and Warnatz, J., 1990, "A Detailed Low-Temperature Reaction Mechanism of n-Heptane Auto-Ignition," *The International Symposium on Diagnostics and Modeling of Combustion in Internal Combustion Engines* (*COMODIA 90*), pp. 93~97.

Christensen, M., Einewall, P. and Johansson, B., 1997, "Homogeneous Charge Compression Ignition (HCCI) Using Isooctane, Ethanol and Natural Gas — A Comparison With Spark-Ignition Operation," SAE Paper 972874.

Curran, H. J., Gaffuri, P., Pitz, W. J. and Westbrook, C. K., 1998a, "A Comprehensive Modeling Study of n-Heptane Oxidation, Combustion and Flame," Vol. 114, pp. 149~177.

Curran, H. J., Gaffuri, P., Pitz, W. J. and Westbrook, C. K., 2002, "A Comprehensive Modeling Study of iso-Octane Oxidation," *Combustion and Flame*, Vol. 129, pp. 253~280.

Curran, H. J., P., Pitz, W. J., Westbrook, C. K., Callahan, C. V. and Dryer, F. L., 1998b, "Oxidation of Automotive Primary Reference Fuels at Elevated Pressures," *Proc. Combust. Inst.*, 27, pp. 379~387.

Eng, J. A., Leppard, W. A. and Sloane, T. M., 2002, "The Effects of POx on the Autoignition Chemistry of n-Heptane and Isooctane in an HCCI Engine," SAE paper 2002-01-2861.

Gaydon, A. G., 1957, *The Spectroscopy of Flame, London*, Chapman and Hall Ltd.

Hiraya, K., Hasegawa, K., Urushihara, T., Iiyama, A. and Itoh, T., 2002, "A Study on Gasoline Fueled Compression Ignition Engine — A Trial of Operation Region Expansion —," SAE paper 2002-01-0416.

Inoue, K., Takei, K., Yoshida, K. and Shoji, H., 2000, "Effect of EGR-Induced Hot Residual Gas on Combustion when Operating a Two-Stroke Engine on Alcohol Fuels," *SAE 2000 Transactions Section 4*, Vol. 109, pp. 3067~3080.

Ishibashi, Y. and Asai, M., 1996, "Improving the Exhaust Emissions of Two-Stroke Engines by Applying the Activated Radical Combustion," SAE paper 960742.

Kaneko, M., Morikawa, K., Itoh, J. and Saishu, Y., 2001, "Study on Homogeneous Charge Compression Ignition Gasoline Engine," *The Fifth International Symposium on Diagnostics and Modeling of Combustion in Internal Combustion Engines* (*COMODIA 2001*), pp. 441~446.

Kim, S. W. and Moriyoshi, Y., 2004, "Analysis of Compression Ignition Combustion in a Schnurle-Type Gasoline Engine — Comparison of Performance Between Direct Injection and Port Injection Systems —," *KSME International Journal*, Vol. 18, No. 8, pp. 1451~1460.

Lee, K. H., Gopalakrishnan, V. and Abraham, J., 2004, "An Investigation of The Effect of Changes in Engine Operating Conditions on Ignition in an HCCI Engine," *KSME International Journal*, Vol. 18, No. 10, pp. 1809~1818.

Onishi, S., Jo, S. H., Shoda, K., Jo, D. P. and Kato, S., 1979, "Active Thermo-Atmosphere Combustion (ATAC) A New Combustion Process for Internal Combustion Engines," SAE paper 790501.

Pilling, M. J. (Editor), et al., 1997, "Comprehensive Chemical Kinetics Vol. 35. Low-Temperature Combustion and Autoignition," *Elsevier*, Amsterdam.

Shoji, H., Saima, A., Shiino, K. and Ikeda, S., 1992, "Clarification of Abnormal Combustion in

a Spark Ignition Engine," SAE Paper 922369.

Shoji, H., Saima, A. and Shiino, K., 1993, "Simultaneous Measurement of Light Emission and Absorption Behavior of Unburned Gas During Knocking Operation," SAE Paper 932754.

Suzuki, T., Ohara, H., Kakishima, A., Yoshida, K. and Shoji, H., 2003, "A Study of Knocking Using Ion Current and Light Emission," *SAE 2003 Transactions Section 3*, Vol. 112, pp. 2058~

2065.

Thring, R. H., 1989, "Homogeneous Charge Compression-Ignition (HCCI) Engines," SAE paper 892068.

Warnatz, J., Mass, U. and Dibble, R., 2001, *Combustion 3rd Edition*, Springer.

Willand, J., Nieberding, R., Vent, G. and Enderle, C., 1998, "The Knocking Syndrome Its Cure and Its Potential," SAE paper 982483.